Vol. 153: 17–29, 2023
https://doi.org/10.3354/dao03716

DISEASES OF AQUATIC ORGANISMS
Dis Aquat Org

Published February 2

Mass mortality of collector urchins *Tripneustes gratilla* in Hawai`i

Thierry M. Work[1,*], Julie Dagenais[1], Bob Rameyer[1], Renee Breeden[1], Tina M. Weatherby[2]

[1]US Geological Survey, National Wildlife Health Center, Honolulu Field Station, Honolulu, Hawai`i, USA
[2]University of Hawai`i, Pacific Biomedical Research Center, Honolulu, Hawai`i, USA

ABSTRACT: As grazers, sea urchins are keystone species in tropical marine ecosystems, and their loss can have important ecological ramifications. Die-offs of urchins are frequently described, but their causes are often unclear, in part because systematic examinations of animal tissues at gross and microscopic level are not done. In some areas, urchins are being employed to control invasive marine algae. Here, we describe the pathology of a mortality event in *Tripneustes gratilla* in Hawai`i where urchins were translocated to control invasive algae. Although we did not determine the cause of the mortality event, our investigation indicates that animals died from inflammation of the test and epidermal ulceration, followed by inability to maintain coelomic fluid volume, colonization of coelomic fluid by opportunists (diatom, algae), and inappetence. Parasites, bacteria, fungi, and viruses were not evident as a primary cause of death. Pathology was suggestive of a toxin or other environmental cause such as lack of food, possibilities that could be pursued in future investigations. These findings highlight the need for caution and additional tools to better assess health when translocating marine invertebrates to ensure maximal biosecurity.

KEY WORDS: Echinoderm · Pathology · Translocation · Epizootic

1. INTRODUCTION

In tropical marine ecosystems, sea urchins play an important role as grazers by helping maintain a balance between fast growing macroalgae and more slowly growing coral reefs (Ogden & Lobel 1978). Because of this, extirpation of urchins from some coral reefs can have profound adverse ecological consequences. A classic illustration of this was unexplained mortalities of *Diadema antillarum* that led to >90% declines of urchins over a year throughout the entire Caribbean (Lessios 2016). Concomitant with this urchin mortality, additional insults such as progressive algal overgrowth, widespread coral disease, bleaching events and overfishing led to secular declines over time in the dominant genus of coral *Acropora* over the ensuing decades; corals and urchins have yet to recover (Aronson & Precht 2001, Jackson et al. 2001, Lessios 2016). The cause of the *Diadema* mortality was never determined mainly because no samples were taken for laboratory testing (Lessios 2016).

Since that event, several efforts have been taken to better understand causes of mortality in sea urchins (Wang et al. 2013). Most die-offs are assumed to be caused by infectious diseases, usually bacteria, based mainly on presence of clinical signs, microbial cultures, and molecular studies (Tajima et al. 1998, Nagelkerken et al. 1999, Becker et al. 2007, Clemente et al. 2014, Sweet et al. 2016). Other die-offs have been associated with environmental changes such as a mass mortality of *Paracentrotus lividus* in Spain associated with elevated seawater temperatures (Girard et al. 2012). Studies that focus on care-

*Corresponding author: thierry_work@usgs.gov

Publisher: Inter-Research · www.int-res.com

ful examination of morphology of urchin tissues at the gross and microscopic level provide a systematic framework to exclude potential causes of death in animals (Work & Meteyer 2014); however, such studies are less common. Moreover, understanding changes in host tissues at the cellular level might yield important insights into the anatomic and physiologic processes that leads to mortality. A good example where such approaches have yielded important understanding of etiology, pathogenesis, and pathophysiology of urchin disease is parameobiasis, a parasitic disease of *Strongylocentrotus droebachiensis*, in Canada that is probably one of the most comprehensively described urchin diseases (Scheibling & Hatcher 2013). Shimizu (1994) used histology to describe an inflammatory response associated with worm infection in the gonads of *Strongylocentrotus intermedius* in Japan. In some cases, systematic approaches to investigating urchin lesions using microscopic examinations do not always yield a cause of death. However, such investigations are valuable to help rule out infectious agents as causes of lesions thereby providing more focused avenues of investigations moving forward. They also provide insights on the process leading to death of the animal. For instance, Roberts-Regan et al. (1988) described pathogenesis of test lesions in *S. droebachiensis* that were sometimes associated with bacteria. In a more recent example, a pathology investigation of a mortality event in *Tripneustes ventricosus* in St. Kitts showed inflammation of multiple organs that could not be traced to infectious agents leading the authors to suggest perhaps a toxin or virus could be involved (Virwani et al. 2021).

The recognition that sea urchins play an important role in coral reefs has led to their use as a management tool to reduce abundances of invasive algae. Since 2010, the State of Hawai`i has used the abundant native collector urchin *Tripneustes gratilla* to control several species of invasive algae in patch reefs of Kaneohe Bay (KB), Oahu (Stimson et al. 2001, Westbrook et al. 2015). In this program, invasive algae are mechanically removed from coral reefs, and then urchins (at the time, mostly captured in the wild from other locations on Oahu, with a minority raised in captivity) are released in the newly cleared patches with the aim of keeping algae under control. In 2014, urchins at one of the collection sites on southeast Oahu manifested loss of spines and epidermal ulceration. Subsequently, urchins at the release site in KB manifested similar clinical signs, and reports of dying urchins were also received from Maui during a similar time frame. Our objective was to describe the temporal course of events, demographics, clinical observations, gross findings, and histopathology of this *T. gratilla* mortality event.

2. MATERIALS AND METHODS

2.1. Field surveys and scoring

On 27 January 2014, urchins were collected from a submerged barge in Maunalua Bay (MB) on SE Oahu for relocation to KB to the northeast (Fig. 1). On 1 February 2014, numbers of urchins were noted to be declining at the barge, but animals were translocated from the barge in MB to KB 2 days later. On 19 February 2014, urchins manifesting loss of spines and epidermal ulceration of the test were seen at the barge in MB, and on 24 February 2014, urchins manifesting lesions similar to those seen at the barge were found in KB (Fig. 1). Two hundred and thirty urchins that had originally been translocated from the barge in MB to KB were removed from KB and placed permanently into flow-through seawater tanks at Sea Life Park Aquarium located on Southwest Oahu on 26 February 2014 and 3 March 2014. Despite this intervention, sick urchins continued to be found in KB to the south of the release site through 6 May 2014 (Fig. 1). On June 2014, reports of sick and dying urchins at Honolua, Maui prompted

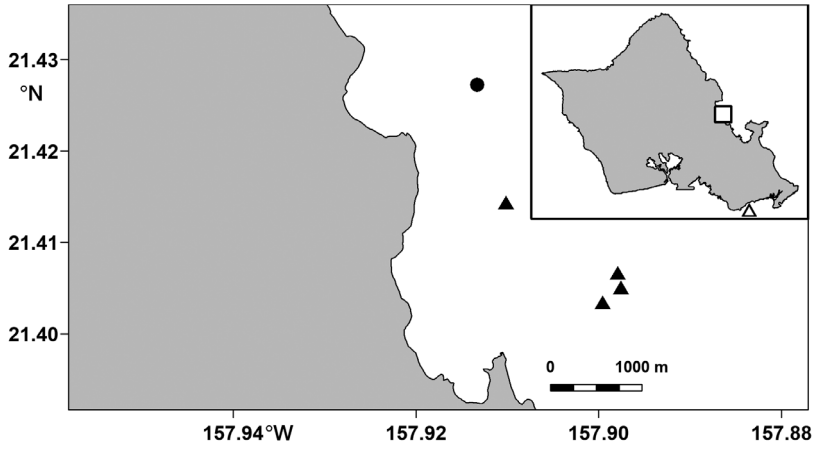

Fig. 1. Outbreak locations of *T. gratilla* mortalities in Oahu. Inset is map of Oahu island, ▲ on SE shore: original outbreak location (1 February 2014); □: location of Kanehoe Bay. Main map is Kanehoe Bay, ●: release site location; ▲: location of sick urchins initially detected after release

surveys at Honolua, Honokawai, Olowalu, Ma`alea, Kaeawakapu, and Makena. Sick *Tripneustes gratilla* were only seen at SE Honolua Bay. On 3 July 2014, we received reports of sick urchins at Mahukona (west Hawai`i), but a 2-day field investigation there failed to reveal urchins with gross lesions. However, empty skeletons (tests) of dead urchins were seen during dive surveys.

A variety of survey techniques were used to assess prevalence of disease and population responses to the mortality event. To assess prevalence (percent) of animals with lesions in KB, teams of divers swam over 3 patch reefs and enumerated animals with and without lesions on 6 and 28 May 2014. To assess long term effects of mortality on urchin populations, surveys were done using one 30 × 2 m transect on SE Oahu at the barge (the site of the initial outbreak) and a location called Z-blocks situated ca. 500 m to the SE. Two surveys were done in 2014 and follow up monthly surveys were done in 2016. Surveys were not done in 2015 due to lack of access to those sites. To assess prevalence of lesions in Honolua Maui, we surveyed a single transect measuring 25 × 2 m at each site during each survey in June 2014. Roving diver surveys were used to assess lesioned urchins in Mahukona, west Hawai`i in June 2014.

2.2. Pathology

Live moribund urchins, as determined by visible movement of teeth in lantern or active movement of spines, were collected by hand using SCUBA or snorkel. Prior to necropsy, animals were photographed orally and aborally and were subjectively assigned a gross lesion score based on severity of spine loss as 0 (healthy), 1 (mild), 2 (moderate) or 3 (severe) (Fig. 2A–H). Specifically, Score 0 urchins were those with vigorously moving spines with white tips, extended tube feet, and often with objects (pieces of rubble, shell fragments) held on top of the urchin with pedicellariae (characterizing these animals as collector urchins). Score 1 urchins had dull spines often flattened or attenuated with absence of extended tube feet. Score 2 urchins were as in Score 1 with evidence of mild focal to multifocal ulceration. Score 3 urchins had diffuse denudation or attenuation of spines with ulceration. Test diameter was measured to the nearest 0.1 cm using calipers and animals were weighed (gross weight) to the nearest gram. Coelomic fluid was drained by puncturing the peristomial membrane, and animals were again weighed (net weight). Percent weight as coelomic fluid was calculated as follows: (gross – net)/gross. Fill of the gut with algae was scored subjectively as 2 (large amounts of algae), 1 (trace amounts of algae) or 0 (no visible contents) (Fig. 2J–P). Drops of coelomic fluid were placed on microscope slides, allowed to air dry, stained with Wright/Giemsa (Hema 3, Thermo-Fisher, Waltham, MA) according to manufacturer instructions, and the smears examined for presence of intracellular or extracellular organisms. Ceolomocytes were not quantified, because standardized methods to evaluate hematology for *T. gratilla* were not established until after this outbreak (Work et al. 2020). Sections of the gonad, gut, peristomial membrane, lantern and associated muscles, oral and aboral test comprising ambulacral and interambulacral regions were saved in 10% formalin. For histology processing, calcified tissues were decalcified overnight in formic acid (Cal ex II, Thermo-Fisher) prior to embedding in paraffin, sectioning at 5 µm, and staining with hematoxylin and eosin (HE; Thermo-Fisher). For the test, severity of coleomocyte infiltrates were subjectively scored as 0, 1, 2, or 3 (none, mild, moderate, severe) (Fig. 2M–P). All histology slides were read blind with no knowledge of gross lesion score category. Special stains (Thermo-Fisher) used included Giemsa to detect protozoa, and periodic-acid-Schiff's reaction (PAS) to see if the large granules in the large eosinophilic coelomocytes consisted of polysaccharides (Prophet et al. 1992).

For electron microscopy, tests showing infiltrates of large eosinophilic cells were preserved in modified Karnovsky's fixative (Karnovsky 1965) made with artificial seawater and decalcified in EDTA. Tissues were rinsed in 0.1 M sodium cacodylate buffer containing 0.35 M sucrose and postfixed with 1% osmium tetroxide in 0.1 M sodium cacodylate buffer. Tissue was dehydrated in a graded ethanol series, then embedded in LX112 epoxy resin. Epoxy-embedded tissues were cut into 1 µm thick sections and stained with Richardson's stain for light microscopy. Ultrathin (60 to 80 nm) sections were obtained on an RMC Powertome ultramicrotome, double stained with uranyl acetate and lead citrate, viewed on a Hitachi HT7700 transmission electron microscope (TEM) at 100 kV, and photographed with an AMT XR-41B 2k-by-2k charge-coupled device camera. Electron microscopy was done at the University of Hawai`i Biological Electron Microscope Facility, Honolulu, Hawai`i.

Electron-microscopy findings were suggestive of intracellular structures compatible with either filamentous viral-like particles or tubulin. Feulgen's stain

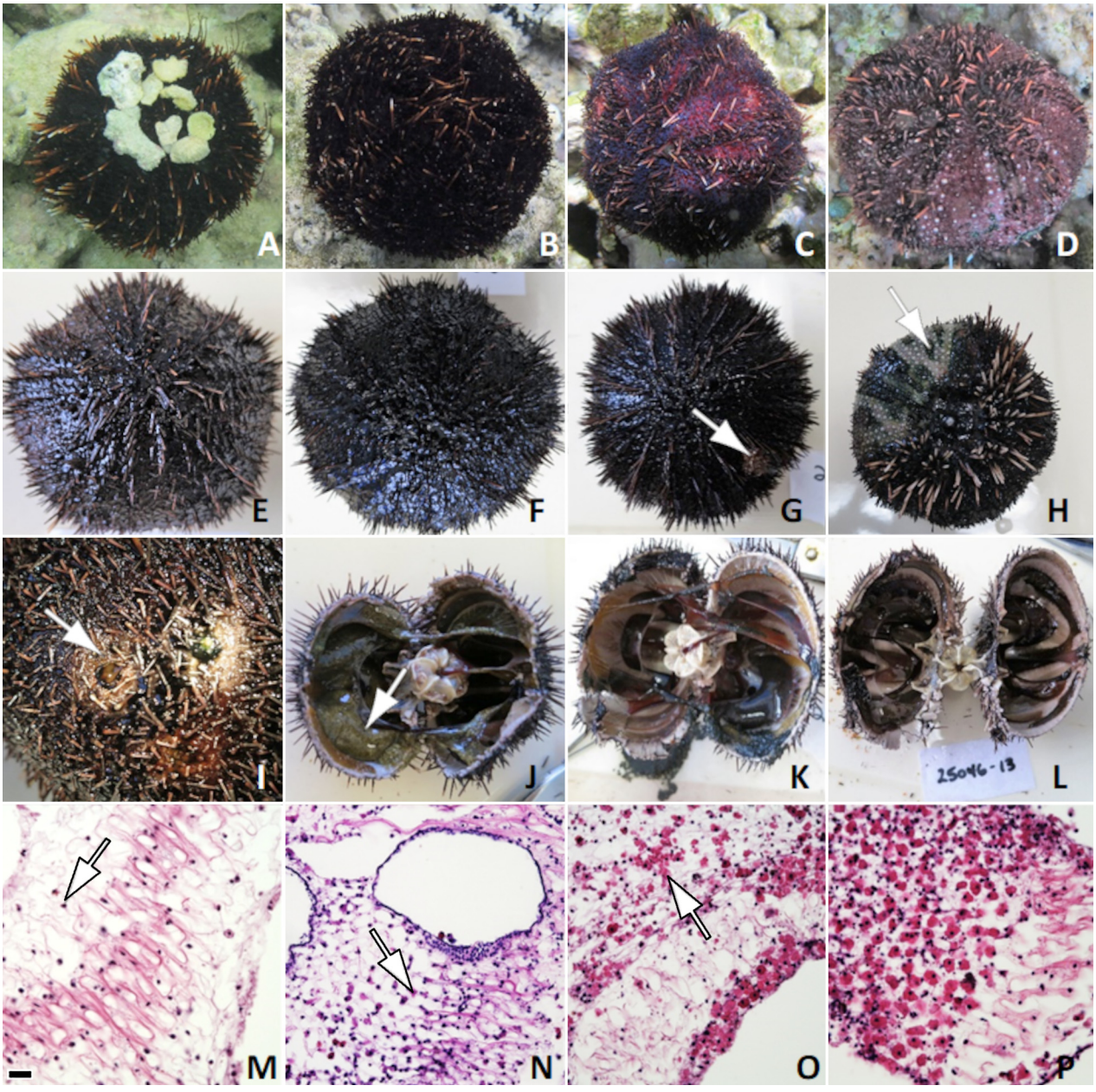

Fig. 2. *Tripneustes gratilla* gross lesion severity scores *in situ* (A–H), *ex situ* (E–H), ulcer (I), gut fill scores (J–L), and test inflammation severity scores (M–P). (A,E) Score 0: unaffected — extended tube feet, spines with white tips, and debris collected on top of urchin, indicating ability of pedicellariae to prehend materials. (B,F) Score 1: mildly affected — dullness and flattening of spines and attenuation of tube feet. (C,G) Score 2: moderately affected — as in Score 1 with focal ulceration (arrow). (D,H) Score 3: severely affected — as in Score 2 but with diffuse loss of spines and epidermis, revealing underlying test with multifocal ulceration (arrow). (I) Close up of 2 ulcers (arrow). (J) Full gut (Score 2): all gut loops replete with algae (arrow). (K) Partially full gut (Score 1): mostly empty gut with small amounts of algae (arrow). (L) Empty gut (Score 0): gut bereft of algae. (M) Score 0 test: stereom composed of organic collagenous matrix intermixed with minerals and scattered coelomocytes (arrow). (N) Score 1 test: mild infiltrates of large granular coelomocytes (arrow); large cavity lined by cells: water vascular canal. (O) Score 2 test: moderate infiltrates of large granular coelomocytes (arrow). (P) Score 3 test: stereom effaced by infiltrates of large granular coelomocytes. Scale bar in panel M (also applies to panels N–P) = 25 µm

and methyl green pyronin were used to see if these structures contained DNA or RNA, respectively, with urchin gut as positive controls (Prophet et al. 1992). We assayed for tubulin using immunohistochemistry (IHC) and western blot containing rabbit polyclonal anti-tubulin ab15568 antibodies (Abcam, Boston, MA).

For IHC, tissues were deparaffinized with xylene and rehydrated in ethanol series 100%, 95%, followed by equilibration in Tris buffer. Antigens were retrieved by heating tissues at 90°C for 10 min in 10 mM citrate buffer pH 6 and endogenous peroxidases blocked with 3% H_2O_2 for 5 min. After washing with Tris buffer, tissues were blocked with 10% goat serum in phosphate-buffered saline for 1 h at room temperature. Tissues were then incubated with anti-tubulin antibody at 1:200, 1:500, and 1:1000 overnight. After 3 washes in Tris buffer, secondary antibodies conjugated to horseradish peroxidase (HRP) were applied (Vector Labs, Newark, CA), and tissues washed again 3 times. Color development was done with diaminobenzidine, tissues counterstained with hematoxylin, and mounted for microscopic examination. Urchin testes were used as positive controls because sperm are a rich source of tubulin (Mohri 1968). Negative controls were treated as above, minus incubation with primary anti-tubulin antibodies.

For Western blot, 0.3 g tests were homogenized in 1 ml lysis buffer (0.025 M Tris, 0.15 M NaCl, 0.001 M EDTA, 1% NP-40, 5% glycerol, pH 7.4) on ice with 3.6 µl protease inhibitor (Sigma), centrifuged at 13 000 × *g* for 10 min in a refrigerated centrifuge, decanted, and proteins quantified with Pierce BCA assay (Thermo-Fisher). Homogenates (20 µg protein per well) were resolved on denaturing reducing electrophoresis on 10% gels, and proteins transferred to nitrocellulose membranes. Membranes were blocked with 5% non-fat dried milk in Tris buffer for 1 h, washed 3 times, probed with rabbit anti-tubulin (Abcam, Waltham, MA) at 1:1000 in 3% milk-Tris buffer overnight at 4°C, washed 3 times, and incubated with HRP-conjugated goat-anti-rabbit polyclonal antibodies (Southern Biotech) diluted 1:1000 in 3% milk-Tris buffer for 1 h. After 3 washes, membrane was incubated with diaminobenzidine. Positive control was HeLa cell lysates as recommended by the antibody manufacturer (Abcam).

2.3. Statistics

We used chi-square test to compare test inflammation scores between oral and aboral tests for animals where both regions were sampled. We used ordinal regression to see if test inflammation score, gut fill score, test diameter, and percent coelomic fluid volume differed significantly ($p < 0.05$) among gross lesion severity score categories. All analyses were done with R Version 4.0.5 (R Core Team 2017) using the MASS package (Venables & Ripley 2002).

3. RESULTS

3.1. Field surveys and scoring

On 6 May 2014, 60 of 2070 (3%) *Tripneustes gratilla* had lesions on 3 patch reefs surveyed in KB. Follow up surveys on 28 May 2014 revealed 16 of 1520 (1%) urchins with lesions. Numbers of urchins at the original outbreak site (barge) declined during the outbreak and numbers remained low thereafter, whereas numbers at nearby Z-blocks were invariant in 2016 (Fig. 3). In Honolua Maui, 3 of 686 (0.4%) urchins had lesions. No sick urchins were seen in other locations on Maui or in west Hawai`i. No other echinoderms including *Heterocentrotus mamillatus, Echinometra mathaei, Echinometra oblonga, Echinostrephus aciculatus, Echinothrix diadema, Echinothrix calamaris*, and *Pseudoboletia indiana* had lesions.

3.2. Pathology

Of the eighty-four urchins necropsied, 26 (31%), 19 (23%), 16 (19%), and 23 (27%) were given gross lesions scores of 0, 1, 2, or 3, respectively. No ulcers were present in Score 0 or 1 animals, whereas ulceration was present in 4 of 16 (25%) Score 2 urchins

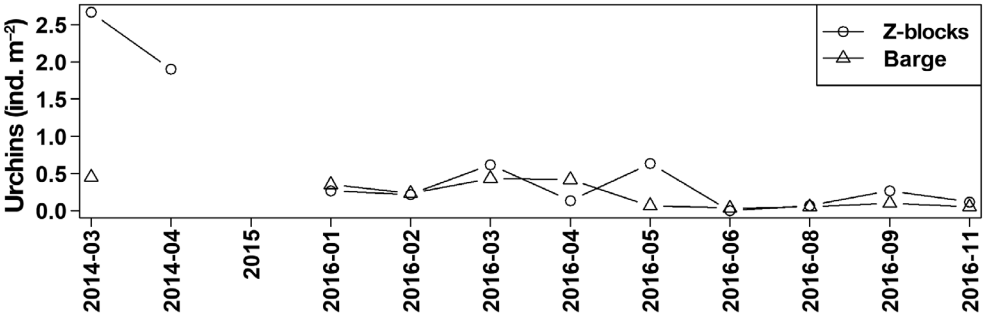

Fig. 3. Urchins density at the outbreak site (Barge) and nearby Z-blocks in 2014 and 2016. *x*-axis is year-month of survey. No data were collected in 2015

and 18 of 23 (78%) Score 3 urchins. Ulceration ranged from diffuse ablation of epidermis (Fig. 2H) to localized holes with green pigmentation in the test bordered by denuded epidermis (Fig. 2I). Coelomic fluid of 5 animals (2 with gross lesion score 0, 1 with gross lesion score 2, and 2 with gross lesion score 3) had bacteria (Fig. 4A), 2 animals (gross lesion score 0 and 3) had diatoms (Fig. 4B,C), and 1 animal (gross lesion score 0) had algae (Fig. 4D). Tissues examined histologically included (N = number of animals) test, gut, gonad (N = 84 each), peristomial membrane (N = 35), water vascular canal (N = 31), nerve ring (N = 25), tube feet (N = 21), axial organ (N = 9), and lantern and associated muscles (N = 6). Microscopically, lesions were most often seen in the test, gut, or testes (Table 1). The most common lesion in the test was varying degrees of inflammation comprising large granular cells with plump red cytoplasm on HE staining (Fig. 2N,O) that were about twice the size of host-derived red spherule cells (Fig. 5A). Large granular cells stained positive for PAS (Fig. 5B), but negative with Feulgen's stain (Fig. 5C,D), methyl green pyronin (Fig. 5E,F), and Giemsa. Cytoplasm of large granular cells immuno-stained positive for tubulin; however, background staining was heavy for the test tissues, complicating interpretation of tubulin localization to inflammatory cells and making these findings non-contributory (Fig. S1A in the Supplement at www.int-res.com/articles/suppl/d153p017_supp.pdf). Conversely, testes provided good contrast with sperm tails' immuno-staining clearly positive for tubulin contrasting (Fig. S1B). Western blot of positive control HeLa cell homogenates showed a distinct band at the expected molecular weight of 55 kDa for tubulin, and a similar but much weaker band for urchin test homogenates (Fig. S1C).

Other changes seen microscopically included lysis of test stereom (Table 1) differentiated from normal vascular water vascular canals lined by cuboidal epithelium (Fig. 6A). Occasionally, algae were seen infiltrating test stereom associated with necrosis (Fig. 6B). Rarely (Table 1), amorphous concretions were present in otherwise normally appearing test stereom (Fig. 6C). Other changes seen included presence of ciliate in the lumen of the gut (Fig. 6D), intracytoplasmic cuboidal inclusions in nuclei and cytoplasm of gut mucosal cells (Fig. 6E), rare infiltrates of

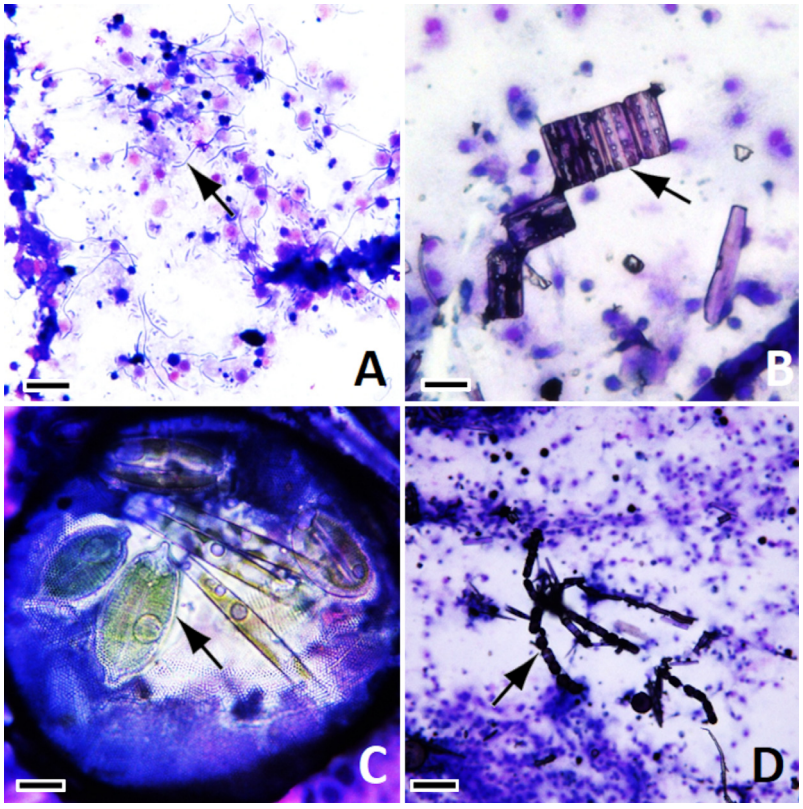

Fig. 4. Coelomic fluid from *Tripneustes gratilla* stained with Wright stain. (A) Filamentous bacteria (arrow) among coelomocytes in a gross lesion score 3 urchin. (B,C) Diatoms (arrow) in a gross lesion score 0 urchin. (D) Algae (arrow) in a gross lesion score 3 urchin. Scale bars = (A,D) 10 µm, (B,C) 5 µm

Table 1. Histologic lesions for 84 *Tripneustes gratilla* categorized by gross lesion scores and by organ. 0: no gross lesions; 1: mild; 2: moderate; 3: severe spine loss; N: number of individuals; (% of the same score)

	Score 0	Score 1	Score 2	Score 3
N for each score	26	19	16	23
Test				
Inflammation	21 (81)	16 (84)	16 (100)	17 (74)
Ossicle lysis	8 (31)	2 (11)	9 (56)	7 (30)
Necrosis with algae	0 (0)	0 (0)	1 (6)	2 (9)
Concretions	0 (0)	2 (11)	0 (0)	0 (0)
Gut				
Intraluminal ciliates	0 (0)	2 (11)	2 (12)	5 (22)
Cuboidal inclusions	4 (15)	1 (5)	1 (6)	0 (0)
Inflammation	1 (4)	0 (0)	0 (0)	0 (0)
Testes				
Presence of algae	0 (0)	0 (0)	0 (0)	2 (9)

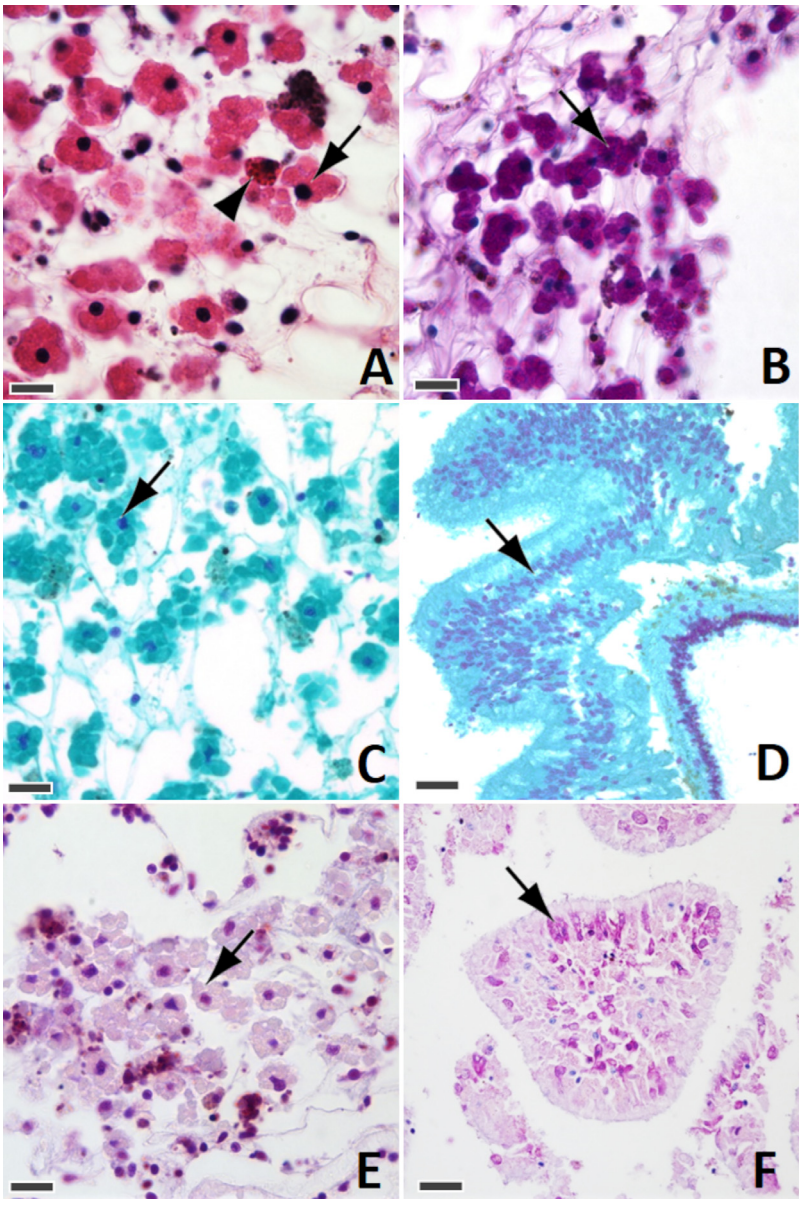

Fig. 5. Inflammatory cells in test of *Tripneustes gratilla* under different stains. (A) hematoxylin and eosin (HE): large granular cells (arrow) distinct from host inflammatory cells such as red spherule cells (arrowhead). (B) periodic-acid-Schiff's reaction (PAS): large granular cells (arrow) staining positive with PAS. (C) Feulgen's stain: negative staining of granular cells cytoplasm in contrast with darker staining nucleus indicating DNA (arrow). (D) Feulgen's stain of urchin gut: positive control, darkly staining blue nuclei (arrow). (E) methyl green pyronin (MGP), negative staining of granular cells cytoplasm (arrow). (F) MGP stain of gut: positive control, pink perinuclear intracytoplasmic coloration (arrow) indicative of RNA. Scale bars = (A–C,E) 20 µm, (D,F) 40 µm

coelomocytes in gut mucosa, and invasion of testes by algae (Fig. 6F) (Table 1).

Electron microscopy of large eosinophilic inflammatory cells in the test showed them to be distended with intracytoplasmic accumulations of variably sized tubules without a core and of variable electron density (Fig. 7A), measuring about 90 nm in diameter, and often associated with membranes (possibly lysosomes) (Fig. 7B). Inclusions in nuclei of gut cells (Fig. 7C) were square or rhomboid, and composed of arrays of small dots (Fig. 7D).

3.3. Statistics

Although the total histology inflammation severity score for oral test (71) was about 50% higher than that for aboral test (48), the relationship between severity scores between aboral and oral test by Fischer's exact test was not significant ($p > 0.05$). Ordinal regression revealed that gross lesion severity score significantly influenced percent weight coelomic fluid and gut fill score, whereas no significant relationship existed for test inflammation score or test diameter (Fig. 8, Table S1). With increasing gross lesion score, more animals with empty guts were observed, and percent coelomic fluid increased (Fig. 8).

4. DISCUSSION

The causes of most urchin mortalities published in the literature remain enigmatic. Although microorganisms like bacteria are commonly implicated as causes of urchin deaths (Wang et al. 2013), diagnostic efforts to confirm this in the form of systematic exams of tissues at the microscopic level are uncommon. Williams et al. (1996) documented unusual mortalities of *Tripneustes ventricosus* in Puerto Rico in 1995 with gas-filled urchins floating at the ocean surface and losing their spines. An earlier mortality of the same species in the same region in 1993 manifesting loss of spines was attributed to increased water temperature (Colon-Jones 1993) and in 1968, again in Puerto Rico, Glynn (1968) documented mortalities of *T. ventricosus* associated with low tides and excessive high water temperature. In

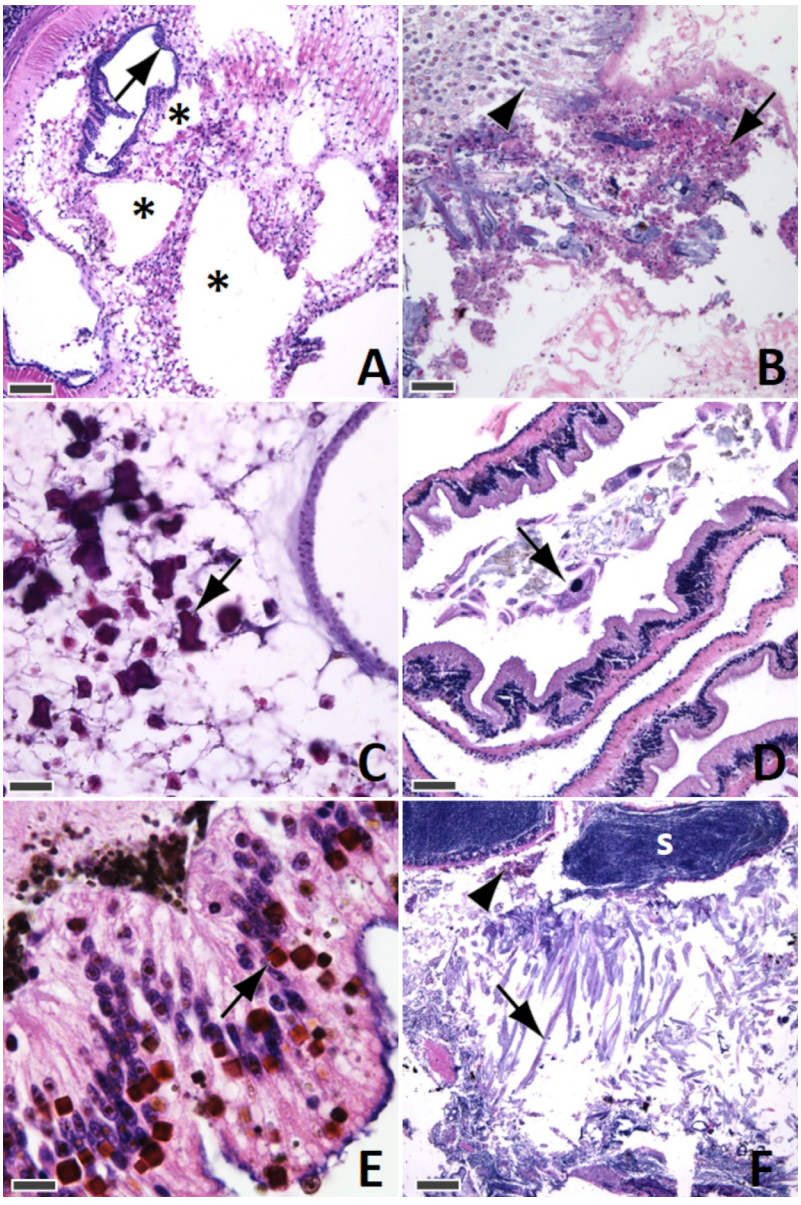

Fig. 6. Other changes observed microscopically. (A) Lytic areas of test stereom: large irregular lacunae (asterisk) lined by inflammatory cells-infiltrated stereom; normal water vascular canal network lined by cuboidal epithelium (arrow). (B) Necrosis of test stereom with algal infiltrates: clumps of cellular debris (arrow) associated with infiltrates of parallel-arranged filamentous structures with thick cell walls (arrowhead) and stereom to lower right. (C) Concretions within stereom: variably sized irregular basophilic structures with angular borders in the stereom matrix (arrow), water vascular canal lined by cuboidal epithelium on the right. (D) Large ciliates (arrow) within gut lumen. (E) Variably sized cuboidal inclusions within cytoplasm of otherwise unremarkable gut mucosa. (F) Algae invading testes: clusters of spermatozoa (s), clumps of necrotic debris (arrowhead), large numbers of filamentous algae (arrow) effacing testicular architecture. Scale bars = (A,D,F) 50 µm, (B,C,E) 20 µm

the Pacific, Birkeland (1989) documented unusual mortalities of *T. gratilla* that started in Hawai`i in the 1980s and progressed to Maui and Molokai. In none of these cases were tissues of animals systematically examined to ascertain cause of death, leaving little information on the cause of most urchin die-offs. Even with extensive pathological examinations, there are no guarantees that a cause of a mortality event might be evident. For instance, a recent study of unusual mortalities of *T. ventricosus* in St. Kitts employed extensive histopathology and microbiology studies but failed to identify a cause of death (Virwani et al. 2021). However, because of their investigation, those authors were able to rule out infectious agents such as bacteria, parasites, or fungi. Based on their findings Virwani et al. (2021) could also chart a viable path forward for future studies such as looking for contaminants, viruses, or environmental causes, thereby illustrating the benefits of such an approach.

Like Virwani et al. (2021), we were unable to determine the ultimate cause of the 2014 *T. gratilla* die-off despite extensive examinations of tissues. However, our exercise was important because it sheds insights on host responses of *T. gratilla* and pathology in echinoderms from mortality events. Balding and spine loss in sea urchins are non-specific clinical signs illustrating that urchins, like other echinoderms, have a limited host response repertoire, a point made by others (Virwani et al. 2021). For instance, sea star wasting disease manifests as epidermal ulceration, a symptom also associated with temperature anomalies (Aalto et al. 2020) and deposition of organic matter on the surface of the starfish leading to anaerobic conditions and tissue wasting (Aquino et al. 2021, Work et al. 2021). Urchins with more severe gross lesions had higher likelihood of having empty guts and higher volumes of coelomic fluid. Whether empty guts and increased coelomic fluid volume lead to test lesions or vice versa cannot be determined from this study. Without monitoring and sampling sick urchins over time, conclusions on how morbidity progressed and the sequence of lesion development are limited. Moreover, findings in this study did not reveal in-

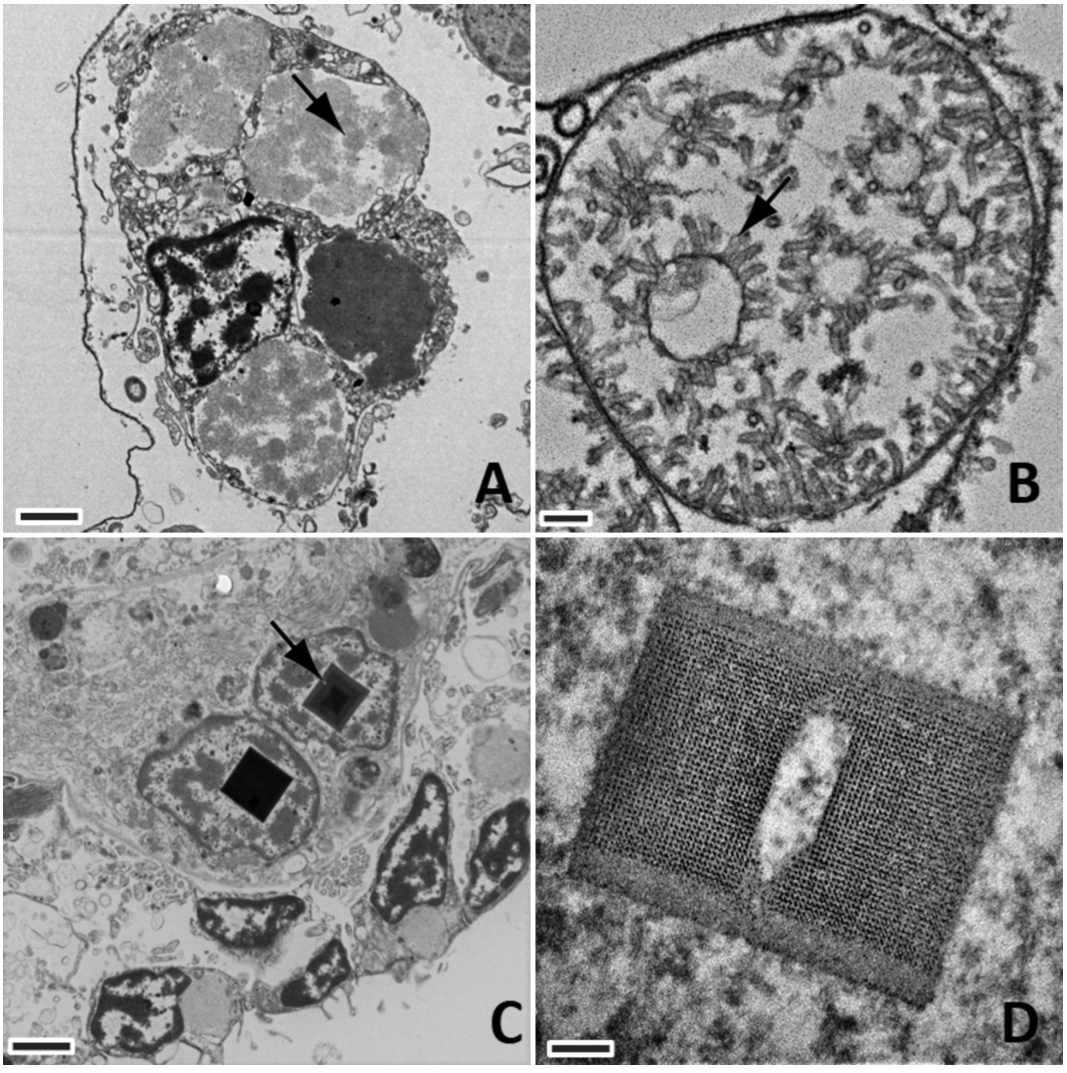

Fig. 7. Transmission electron micrographs of tissues from *Tripneustes gratilla*. (A) Large granular cell within test distended by intracytoplasmic coarse material (arrow). (B) Close up of coarse material: numerous variably sized tubular structures (arrow) associated with circular membranes. (C) Gut cells with cuboidal inclusions (arrow). (D) Close up of inclusion comprised of parallel arrays of small (<1 nm) dots that fade to upper and lower edges and central elongated hexagonal cavity. Scale bars = (A,C) 2 µm, (B) 250 nm, (D) 100 nm

fectious agents (viruses, bacteria, parasites, fungi), at least visible on light and electron microscopy, as responsible for this outbreak, but rather suggests an environmental or potentially toxic cause.

Most of the urchins in this die-off had reduced stomach contents indicating that food limitation might have contributed to this mortality event. In the field, this would presumably be manifested by high density of urchins followed by population crashes. For instance, in kelp forest ecosystems, grazing urchins go through boom-bust cycles with populations increases, overgrazing of kelp, and subsequent population crashes (Scheibling 1986). However, this seems to be an exception, and in general, many echinoderms can maintain very high spatial densities in absence of food for long periods (Andrew 1989). Conversely, in seagrass beds in the Caribbean, *T. ventricosus* converged on a food-limiting density of 1 urchin m^{-2} (Keller 1983). On the island of Hawai`i, densities of *T. gratilla* did not exceed 1 urchin m^{-2} (Ebert 1971). The surveys of the outbreak site and a nearby site in 2014 and 2016 showed a steep decline of urchins at one site (Z blocks) during the time of the outbreak, indicating that the mortality had some measurable demographic effect with no evident recovery of populations. However, densities were well below 0.5 urchins m^{-2}. No survey data was collected prior to the epizootic, so it is impossible to definitively

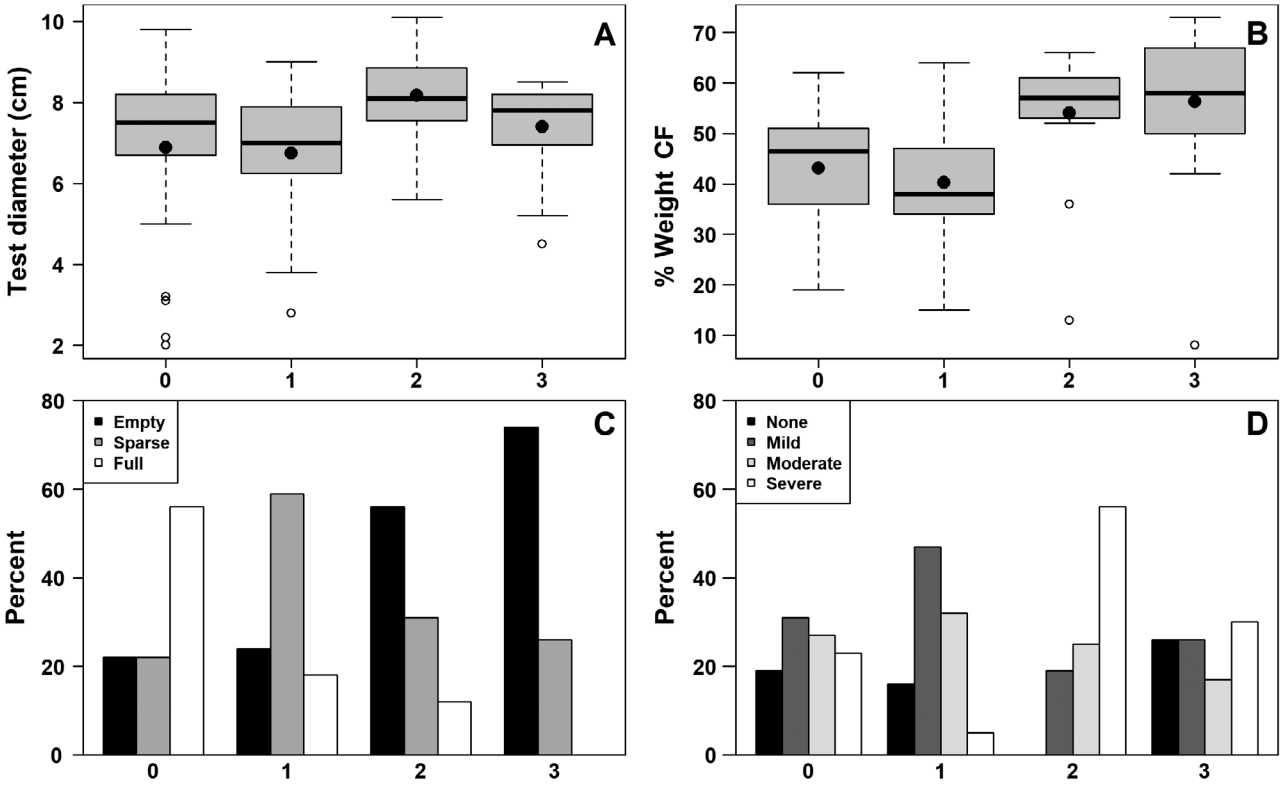

Fig. 8. Morphometrics of 84 *Tripneustes gratilla* vs. gross lesion severity scores 0 (N = 26), 1 (N = 19), 2 (N = 16) and 3 (N = 23). (A) Gut fill score. (B) Percent weight coelomic fluid (CF). Bar: median; ●: mean; boxes: 25th–75th percentiles; whiskers: 1.5 × interquartile range; ○: outlier. (C) Percent of animals with empty, moderately, or filled guts by gross lesion score category. (D) Percent of animals with histology inflammation scores (none, mild, moderate, severe) by gross lesion score category

rule out density-dependence factors as a possible cause of the mortality. Regardless of the cause, it appeared to affect exclusively *T. gratilla* and no other echinoderms, indicating particular behavioral or physiologic attributes of this species make it susceptible to inflammatory lesions in the test.

Urchins with more severe gross lesions had a higher volume of coelomic fluid relative to apparently normal animals. This indicates that sick urchins were unable to modulate coelomic fluid volume. Some aspects of coelomic fluid regulation in echinoderms are known. In the sea star *Pisaster ochraceus*, the madreporite, a specialized structure through which an interchange between seawater and coelomic fluid occurs, is important in maintenance of coelomic fluid volume (Ferguson 1992). When the sea urchins *Lytechinus variegatus, Echinometra lucunter*, and *Arbacia lixula* are immersed in freshwater, the coelomic fluid osmolality decreases (Santos et al. 2013); unfortunately, fluid volume was not measured in that study. In the urchin *L. variegatus*, the movement of the lantern, jaws, and associated muscle are important in circulation of coelomic fluids (Hanson & Gust 1986). Studying *Strongylocentrotus purpuratus*, Ellers & Telford (1992) found that coelomic fluid pressure fluctuated rhythmically and that pressure did not differ between starved and fed urchins; again, fluid volume was not measured. Presumably, higher volume of coelomic fluid in sick urchins would lead to greater pressure, but coelomic fluid pressure was not measured in this study and therefore, no conclusions could be made. Given the epidermal ulceration and inflammation of the test seen in *T. gratilla* in the current study, and considering the aforementioned studies, a combination of madreporite dysfunction and loss of epidermal barrier likely conspired to prevent adequate coelomic fluid regulation in sick urchins. Future studies could examine the madreporite microscopically to see if additional clues can be gained as to the nature of this inability to maintain coelomic fluid balance in sick *T. gratilla*.

About 10% of urchins had foreign organisms in their coelomic fluid including bacteria, diatoms, or other algae visible on light microscopy. Evidence for the sterility of coelomic fluid in echinoderms is mixed. For instance, Unkles (1977) cultured a few bacteria from coelomic fluid of *Echinus esculentus* but judged those to be contaminants from gut flora,

which grew similar bacteria. They hypothesized that accidental needle puncture into the gut was responsible. Urchins such as *S. purpuratus* (Yui & Bayne 1983) and *S. droebachiensis* (Płytycz & Seljelid 1993) can effectively clear bacteria from their coelomic fluid within 24 h, indicating that normal urchins should not have bacteria in coelomic fluid. On the other hand, metagenomic studies revealed bacteria to be common in coelomic fluid of *Paracentrotus lividus* (Faddetta et al. 2020). A hematology survey of 340 apparently healthy *T. gratilla* in Hawai`i failed to reveal bacteria, protozoa, algae, or diatoms detectable by light microscopy (Work et al. 2020), indicating that coelomic fluid of this species is effectively sterile, at least on microscopy. An intact test and epidermis are probably an important innate defense in sea urchins and would normally prevent colonization of coelomic fluid by foreign agents. Possibly, a combination of inability to modulate coelomic fluid volume, epidermal ulceration and test inflammation broke down this innate defense, leading to opportunistic colonization of coelomic fluid by various organisms. Roberts-Regan et al. (1988) saw a similar phenomenon in *S. droebachiensis* of more severe epidermal ulceration of the test leading to more bacterial infections. The finding of organisms in coelomic fluid of apparently normal urchins could have 2 explanations. At the time of the investigations, techniques of blood sampling for urchins were still being perfected, so it was possible that gut may have perforated during sampling. A second explanation is that this study's gross definition of apparently normal urchins may be too crude to capture subtle lesions that could allow for opportunistic colonization of coelomic fluid. A precedent exists in other echinoderms. For instance, microscopic lesions were seen in apparently normal sea stars when epidermal lesions were experimentally induced (Work et al. 2021).

The most substantial microscopic lesions were seen in the test and manifested in varying degrees of inflammation, occasionally associated with algal incursions into urchin tissues. The test comprises 52–67% of the body weight of *T. gratilla* (Bangi & Juinio-Meñez 2019), explaining why pathology is most often seen in this tissue in urchins (Virwani et al. 2021). Roberts-Regan et al. (1988) observed in *S. droebachiensis* more epidermal abrasion in the oral test but had no explanation for this. Although inflammation score in oral test was almost 2 times higher than aboral test, no significant difference was detected. The oral and aboral test of urchins show anatomical and physiological differences. In *S. intermedius*, calcification occurs more rapidly in aboral test (Kobayashi & Taki 1969). In *S. droebachiensis*, oral podia used for walking are thicker than aboral podia which are used for capturing debris (Leddy & Johnson 2000). How these differences could explain tropism for inflammation in oral test of *T. gratilla* is unclear.

In this study, the large granular inflammatory cells seen in *T. gratilla* were distended with large (90 nm diameter) intracytoplasmic tubules that stained negative for DNA and RNA, indicating they were not viruses, but stained positive with PAS, showing presence of polysaccharides (Prophet et al. 1992). The diameter of these tubules (ca. 90 nm) was larger than microtubules (25 nm) (Gall 1966) composed of the protein tubulin, which we found in *T. gratilla* spermatozoa. Whether tubulin was present in inflammatory cells of this study is unclear; however, the protein has been detected in coelomocytes of other urchin species (Edds 1984, D'Andrea-Winslow & Novitski 2008). Intracytoplasmic tubules have been seen by electron microscopy in coelomocytes of other invertebrates, including snails (Matricon-Gondran & Letocart 1999, Martin et al. 2007) and limpets (Harris & Markl 1992), but these were far smaller (25 nm diameter) than what was observed here and were more compatible with microtubules. Electron microscopy of coelomocytes from apparently normal *T. gratilla* sampled after this mortality event failed to reveal such tubules, indicating they are not normal (Work et al. 2020). Given that no evidence of viruses was seen on electron microscopy, future studies might focus on the role of toxins or metabolic abnormalities as the cause of tubular structure accumulation in urchin cells.

Other microscopic changes such as ciliates in the gut and intracytoplasmic inclusions were considered incidental findings. Virwani et al. (2021) saw similar findings in *T. ventricosus* in St. Kitt's that they also considered as incidental. Although it was not confirmed with special stains (Virwani et al. 2021), it is likely that these inclusions are iron crystals, which have been seen in urchins elsewhere (Borges et al. 2010, Branco et al. 2012). Unlike Virwani et al. (2021), no commensal bacterial aggregates were observed in urchins examined in this study.

Although an infectious etiology was not found in this mortality event, and the event did not lead to landscape-scale declines in urchins, it highlights the current lack of knowledge about the health of this important group of organisms. From a disease and biosecurity standpoint, managers might reconsider the practice of translocating urchins with more careful health assessments to ensure that urchins being translocated are as healthy as possible. Gross exami-

nation of animals alone may not be sufficient to assess urchin health as evidenced by the presence of cellular pathology in apparently normal urchins seen here, a phenomenon previously observed in urchins (Virwani et al. 2021) and other marine invertebrates like corals (Landsberg et al. 2020). In addition to potentially moving infectious agents, translocating urchins could lead to introduction of invasive marine algae because algal spores can survive digestion in sea urchins (Santelices et al. 1983). Comprehensive guidelines exist to enhance biosecurity during translocation of invertebrates (Cunningham 1996, Hartley & Sainsbury 2017). Applying these to marine invertebrates in might lead to more successful reintroductions.

Acknowledgments. We thank Hank Lynch from The Nature Conservancy for boat access to Z-blocks and the barge for surveys. Our thanks also to Skippy Hau, Darla White (Hawai`i Department of Aquatic Resources), and Greta Aeby (University of Hawai`i) for assistance during mortality surveys on Maui. Susan Knowles and anonymous reviewers provided constructive comments on earlier versions of this manuscript. Any use of trade, firm, or product names is for descriptive purposes only and does not imply endorsement by the US Government. The PBRC BEMF is supported by NIH NIGMS grants P20GM139753 and P20GM125508. The content is solely the responsibility of the authors and does not necessarily represent the official views of the NIH.

Data availability. Data associated with this study are available at https://doi.org/10.5066/P92DHFO5.

LITERATURE CITED

Aalto EA, Lafferty KD, Sokolow SH, Grewelle RE and others (2020) Models with environmental drivers offer a plausible mechanism for the rapid spread of infectious disease outbreaks in marine organisms. Sci Rep 10:5975

Andrew NL (1989) Contrasting ecological implications of food limitation in sea urchins and herbivorous gastropods. Mar Ecol Prog Ser 51:189–193

Aquino CA, Besemer RM, DeRito CM, Kocian J and others (2021) Evidence that microorganisms at the animal–water interface drive sea star wasting disease. Front Microbiol 11:3278

Aronson RB, Precht WF (2001) White-band disease and the changing face of Caribbean coral reefs. Hydrobiologia 460:25–38

Bangi HGP, Juinio-Meñez MA (2019) Resource allocation trade-offs in the sea urchin *Tripneustes gratilla* under relative storminess and wave exposure. Mar Ecol Prog Ser 608:165–182

Becker P, Gillan DC, Eeckhaut I (2007) Microbiological study of the body wall lesions of the echinoid *Tripneustes gratilla*. Dis Aquat Org 77:73–82

Birkeland C (1989) The influence of echinoderms on coral reef communities. In: Jangoux M, Lawrence JM (eds) Echinoderm Studies, Vol 3. Balkema, Rotterdam, p 1–79

Borges JCS, Branco PC, Pressinotti LN, Severino D, da Silva JRMC (2010) Intranuclear crystalloids of Antarctic sea urchins as a biomarker for oil contamination. Polar Biol 33:843–849

Branco PC, Pressinotti LN, Borges JCS, Lunes RS and others (2012) Cellular biomarkers to elucidate global warming effects on Antarctic sea urchin *Sterechinus neumayeri*. Polar Biol 35:221–229

Clemente S, Lorenzo-Morales J, Mendoza JC, López C and others (2014) Sea urchin *Diadema africanum* mass mortality in the subtropical eastern Atlantic: role of waterborne bacteria in a warming ocean. Mar Ecol Prog Ser 506:1–14

Colon-Jones DE (1993) Size (age) factors controlling the distribution and population size of the white-spined sea urchin, *Tripneustes ventricosus* (Lamark, 1816). MSc thesis, Universidad de Puerto Rico, Mayaguez, Puerto Rico

Cunningham AA (1996) Disease risks of wildlife translocations. Conserv Biol 10:349–353

D'Andrea-Winslow L, Novitski AK (2008) Active bleb formation is abated in *Lytechinus variegatus* red spherule coelomocytes after disruption of acto-myosin contractility. Integr Zool 3:115–122

Ebert TA (1971) A preliminary quantitative survey of the echinoid fauna of Kealakekua and Honaunau Bays, Hawaii. Pac Sci 25:112–131

Edds KT (1984) Differential distribution and function of microtubules and microfilaments in sea urchin coelomocytes. Cytoskeleton 4:269–281

Ellers O, Telford M (1992) Causes and consequences of fluctuating coelomic pressure in sea urchins. Biol Bull 182: 424–434

Faddetta T, Ardizzone F, Faillaci F, Reina C and others (2020) Composition and geographic variation of the bacterial microbiota associated with the coelomic fluid of the sea urchin *Paracentrotus lividus*. Sci Rep 10:21443

Ferguson JC (1992) The Function of the madreporite in body fluid volume maintenance by an intertidal starfish, *Pisaster ochraceus*. Biol Bull 183:482–489

Gall JG (1966) Microtubule fine structure. J Cell Biol 31: 639–643

Girard D, Clemente S, Toledo-Guedes K, Brito A, Hernandez JC (2012) A mass mortality of subtropical intertidal populations of the sea urchin *Paracentrotus lividus*: analysis of potential links with environmental conditions. PSZNI: Mar Ecol 33:377–385

Glynn PW (1968) Mass mortalities of echinoids and other reef flat organisms coincident with midday, low water exposures in Puerto Rico. Mar Biol 1:226–243

Hanson JL, Gust G (1986) Circulation of perivisceral fluid in the sea urchin *Lytechinus variegatus*. Mar Biol 92:125–134

Harris JR, Markl J (1992) Electron microscopy of a double helical tubular filament in keyhole limpet (*Megathura crenulata*) hemolymph. Cell Tissue Res 269:411–420

Hartley M, Sainsbury A (2017) Methods of disease risk analysis in wildlife translocations for conservation purposes. EcoHealth 14:16–29

Jackson JBC, Kirby MX, Berger WH, Bjorndal KA and others (2001) Historical overfishing and the recent collapse of coastal ecosystems. Science 293:629–637

Karnovsky MJ (1965) A formaldehyde-glutaraldehyde fixative of high osmolality for use in electron microscopy. J Cell Biol 27:137A

Keller BD (1983) Coexistence of sea urchins in seagreas meadows: an experimental analysis of competition and predation. Ecology 64:1581–1598

Kobayashi S, Taki J (1969) Calcification in sea urchins. Calcif Tissue Res 4:210–223

Landsberg JH, Kiryu Y, Peters EC, Wilson PW and others (2020) Stony coral tissue loss disease in Florida is associated with disruption of host–zooxanthellae physiology. Front Mar Sci 7:576013

Leddy HA, Johnson AS (2000) Walking versus breathing: mechanical differentiation of sea urchin podia corresponds to functional specialization. Biol Bull 198:88–93

Lessios HA (2016) The great *Diadema antillarum* die-off: 30 years later. Annu Rev Mar Sci 8:267–283

Martin GG, Oakes CT, Tousignant HR, Crabtree H, Yamakawa R (2007) Structure and function of haemocytes in two marine gastropods, *Megathura crenulata* and *Aplysia californica.* J Molluscan Stud 73:355–365

Matricon-Gondran M, Letocart M (1999) Internal defenses of the snail *Biomphalaria glabrata* III. Observations on tubular helical filaments induced in the hemolymph by foreign material. J Invertebr Pathol 74:248–254

Mohri H (1968) Amino-acid composition of 'tubulin' constituting microtubules of sperm flagella. Nature 217: 1053–1054

Nagelkerken I, Smith G, Snelders E, Karel M, James S (1999) Sea urchin *Meoma ventricosa* die-off in Curaçao (Netherland Antilles) associated with a pathogenic bacterium. Dis Aquat Org 38:71–74

Ogden JC, Lobel PS (1978) The role of herbivorous fishes and urchins in coral reef communities. Environ Biol Fishes 3:49–63

Płytycz B, Seljelid R (1993) Bacterial clearance by the sea urchin, *Strongylocentrotus droebachiensis.* Dev Comp Immunol 17:283–289

Prophet EB, Mills B, Arrington JB, Sobin LH (eds) (1992) Laboratory methods in histotechnology. American Registry of Pathology, Washington, DC

R Core Team (2017) R: a language and environment for statistical computing. https://www.R-project.org/

Roberts-Regan DL, Scheibling RE, Jellett JF (1988) Natural and experimentally induced lesions of the body wall of the sea urchin *Strongylocentrotus droebachiensis.* Dis Aquat Org 5:51–62

Santelices B, Correa J, Avila M (1983) Benthic algal spores surviving digestion by sea urchins. J Exp Mar Biol Ecol 70:263–269

Santos IA, Castellano GC, Freire CA (2013) Direct relationship between osmotic and ionic conforming behavior and tissue water regulatory capacity in echinoids. Comp Biochem Physiol A Mol Integr Physiol 164:466–476

Scheibling RE (1986) Increased macroalgal abundance following mass mortalities of sea urchins (*Strongylocentrotus droebachiensis*) along the Atlantic coast of Nova Scotia. Oecologia 68:186–198

Scheibling RE, Hatcher BG (2013) *Strongylocentrotus droebachiensis*. In: Lawrence JM (ed) Sea urchins: biology and ecology. Elsevier, Amsterdam, p 381–412

Shimizu M (1994) Histopathological investigation of the spotted gonad disease in the sea urchin, *Strongylocentrotus intermedius.* J Invertebr Pathol 63:182–187

Stimson J, Larned ST, Conklin E (2001) Effects of herbivory, nutrient levels, and introduced algae on the distribution and abundance of the invasive macroalga *Dictyosphaeria cavernosa* in Kaneohe Bay, Hawaii. Coral Reefs 19:343–357

Sweet M, Bulling M, Williamson JE (2016) New disease outbreak affects two dominant sea urchin species associated with Australian temperate reefs. Mar Ecol Prog Ser 551: 171–183

Tajima K, Shimizu M, Miura K, Ohsaki S, Nishihara Y, Ezura Y (1998) Seasonal fluctuations of *Flexibacter* sp. the causative bacterium of spotting disease of sea urchin *Strongylocentrotus intermedius* in the culturing facilities and coastal area. Fish Sci 64:6–9

Unkles SE (1977) Bacterial flora of the sea urchin *Echinus esculentus.* Appl Environ Microbiol 34:347–350

Venables WN, Ripley BD (2002) Modern applied statistics with S. Springer, New York, NY

Virwani A, Rajeev S, Carmichael-Branford G, Freeman MA, Dennis MM (2021) Gross and microscopic pathology of West Indian sea eggs (*Tripneustes ventricosus*). J Invertebr Pathol 179:107526

Wang YN, Chang YQ, Lawrence JM (2013) Disease in sea urchins. In: Lawrence JM (ed) Sea urchins: biology and ecology. Elsevier, Amsterdam, p 179–186

Westbrook CE, Ringang RR, Cantero SMA, Team HTU, Toonen RJ (2015) Survivorship and feeding preferences among size classes of outplanted sea urchins, *Tripneustes gratilla*, and possible use as biocontrol for invasive alien algae. PeerJ 3:e1235

Williams EH Jr, Bunkley-williams L, Bruckner RJ, Bruckner AW, Ortiz-Corps AR, Bowden-Kerby WA, Colon-Jones DE (1996) Recurring mass mortalities of the white-spined sea urchin, *Tripneustes ventricosus*, (Echinodermata: Echinoidea) in Puerto Rico. Caribb J Sci 32:111–112

Work T, Meteyer C (2014) To understand coral disease, look at coral cells. EcoHealth 11:610–618

Work TM, Millard E, Mariani DB, Weatherby TM and others (2020) Cytology reveals diverse cell morphotypes and cell-in-cell interactions in normal collector sea urchins *Tripneustes gratilla.* Dis Aquat Org 142:63–73

Work TM, Weatherby TM, DeRito CM, Besemer RM, Hewson I (2021) Sea star wasting disease pathology in *Pisaster ochraceus* shows a basal-to-surface process affecting color phenotypes differently. Dis Aquat Org 145:21–33

Yui MA, Bayne C (1983) Echinoderm immunology: bacterial clearance by the sea urchin *Strongylocentrotus purpuratus.* Biol Bull 165:473–486

Editorial responsibility: Jeffrey Shields, Gloucester Point, Virginia, USA
Reviewed by: 3 anonymous referees

Submitted: July 1, 2022
Accepted: December 5, 2022
Proofs received from author(s): January 27, 2023